

LETTER

Quantum weak measurement of Goos–Hänchen effect of light in total internal reflection using a Gaussian-mode laser beam

To cite this article: Akash Das and Manik Pradhan 2020 *Laser Phys. Lett.* **17** 066001

View the [article online](#) for updates and enhancements.

You may also like

- [The Goos–Hänchen shift analysis in optical lattices under the parity-time symmetry](#)
Fazal Badshah, Huma Malik, Anwar Ali et al.
- [Effects of a chiral atomic medium on the manipulation of light birefringence and lateral Goos–Hänchen shifts via Kerr nonlinearity and local field effects](#)
Akhlaq Ahmad, Naeem Jan, Arif Ullah et al.
- [Enhancement and control of the Goos–Hänchen shift by nonlinear surface plasmon resonance in graphene](#)
Qi You, , Leyong Jiang et al.

Letter

Quantum weak measurement of Goos–Hänchen effect of light in total internal reflection using a Gaussian-mode laser beam

Akash Das¹ and Manik Pradhan^{1,2}

¹ Department of Chemical, Biological and Macro-Molecular Sciences, S. N. Bose National Centre for Basic Sciences, Salt Lake City, Kolkata 700 106, India

² Technical Research Centre (TRC), S. N. Bose National Centre for Basic Sciences, Salt Lake City, Kolkata 700 106, India

E-mail: manik.pradhan@bose.res.in

Received 31 October 2019

Accepted for publication 11 April 2020

Published 11 May 2020



CrossMark

Abstract

We report a detailed experimental demonstration of the Goos–Hänchen (GH) shift of light in total internal reflection condition for a Gaussian mode laser beam of 633 nm passing through an air-glass interface. The quantum weak measurement (QWM) technique has been exploited as a weak value amplification scheme to observe the amplified optical GH shift. The amplification of the GH shift depends on the angular deviation from the exact orthogonal position required for weak measurement. We have subsequently investigated the profiles of the beam pattern and their horizontal and vertical shifts in detail. We also show that the beam shift values obtained experimentally agree well with the theoretical results for a specific choice of angle of deviation from the orthogonal condition of weak measurement. Our results clearly demonstrate the advantages of the QWM technique for amplifying and detecting tiny optical beam shift effects and may provide important applications in precision metrology.

Keywords: Goos–Hänchen shift, total internal reflection, Gaussian beam, spatial shift, weak measurement

(Some figures may appear in colour only in the online journal)

1. Introduction

Quantum weak measurement (QWM), a very accurate and promising technique in the context of quantum mechanics, was first introduced and subsequently demonstrated by Aharonov, Albert, and Vaidman (AAV) [1]. The concept of weak measurement can be used as an amplification scheme for the observation of the tiny and weak optical beam shifts. This phenomenon can arise from the weak interaction of the measurement system and the measuring device by an appropriate selection of preselected and post selected states of the system [2, 3]. It is noted that although QWM method has been

proposed in the study of quantum systems [4], it is also widely applied in the framework of classical optics [5, 6]. The optical analog of the QWM concept was first developed by Duck [7] and later, Hosten and Kwiat applied the weak measurement technology in the measurement of tiny spin-Hall effect of the light beam [3].

Recently, there has been an immense research interest to understand the optical beam shift phenomena [8]. The optical beam shifts have potential applications in the field of photonics, plasmonics, optoelectronics, metamaterials, chiral materials, and various other quantum systems [9, 10]. Modifications of the set up has been done to determine layers of

graphene, measure optical conductivity of graphene with high precision, ultrasensitive detection of chemical reaction or ion concentration etc [11–16]. One of the most promising beam shift effects is the Goos–Hänchen (GH) shift of light. A light beam with finite transverse extent does not exactly follow the laws of geometrical optics due to diffractive corrections and induce subtle shifts in both longitudinal (in the plane of incidence) and transverse (out of the plane of incidence) directions [5, 6, 8, 17, 18]. The longitudinal beam shift is known as GH shift—a very tiny shift of the order of the wavelength of the incident light. It is therefore a challenging task to measure such exceedingly small magnitude of the beam shift [8]. Hence, considerable research has been ongoing to measure these tiny beam shifts as precisely as possible [19, 20]. However, using this QWM scheme, the difficulty can be overcome. Among the available techniques [21, 22] to measure optical beam shifts, the QWM technique [3, 6, 14, 20, 23, 24] is a precise and promising method due to its simplicity and ability to largely amplify of the shift values. This technique proves to be an effective and accurate method and offers a new strategy to measure ‘weak value’ by amplifying and detecting a very small beam shift. The details of this technique and the QWM concept have been discussed in the ‘theory’ section.

In this study, we present the experimental demonstrations of the GH effect of light in total internal reflection condition of a calibrated Gaussian-mode laser beam of 633 nm passing through an air-glass interface via weak value amplification scheme. We have developed an experimental QWM set up to demonstrate the amplified GH shift in the total internal reflection (TIR) regime. Here, we have pre-selected the Gaussian beam in a linear polarization basis and post-selected the beam to another linear polarization state nearly orthogonal to the initial state by appropriate arrangement of the optical components in our experimental QWM setup. We have studied the GH shift in the total internal reflection of the light beam at an air-glass interface where the prism serves as the ‘weak measuring device’ in our QWM setup. Though various other beam shifts such as spatial & angular IF shift (transverse), spin hall shift (transverse) may accompany longitudinal GH shift, the current scheme of measurement and optical arrangements only enhance GH shift suppressing others [3, 8, 25, 26]. Here, we have presented the behavior of the spatial shifts with a change in the post-selection states gradually from the orthogonal position. Through the weak measurement scheme, we have shown the continuous change in the shape of the resultant beam along with the horizontal and vertical profiles of the beam, an investigation that has not been explored in any earlier works. The nature of the horizontal and vertical shift of the beam with the angular deviation from the orthogonal position has also been elaborated and the validity of the AAV approximations has been discussed via the weak value amplification scheme. Furthermore, we have also examined the variation of the GH shifts with different angles of incidences and subsequently have compared the results with the previous theoretical results to demonstrate the region of the applicability of the AAV approximations. To the best of our knowledge, a comprehensive investigation of the optical GH effect applying the QWM technique has not been done till date.

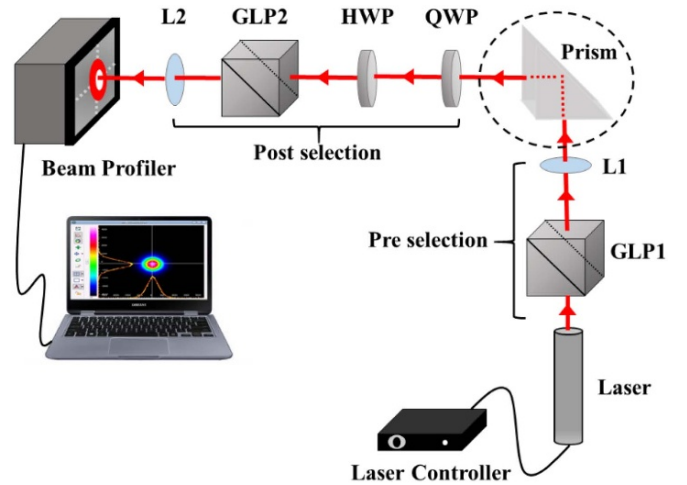


Figure 1. A schematic diagram of the experimental QWM set-up to observe GH shift, where GLP1, GLP2: Glan-Thompson Polarizer; L1, L2: Plano-convex lenses; HWP: Half wave plate; QWP: Quarter wave plate.

2. Theoretical background of QWM

We consider a reflection system as shown in figure 1. An incoming polarized light beam is incident upon a prism. It undergoes TIR at the glass-air interface. The transverse (IF) and longitudinal (GH) shifts of the reflected beam are too small to be detected. Hence, we apply the quantum weak measurement method to optically amplify the beam shifts. To discuss this QWM technique, we consider that the incoming beam is at first pre-selected in an initial quantum state $|\Psi_1\rangle$. The beam then endures reflection from the ‘weak measuring device’ (the prism in our case), where the weak interaction of the incident beam with the glass-air interface takes place. The system is subsequently post-selected in another quantum state $|\Psi_2\rangle$, projected almost orthogonal to the pre-selected state. In this way, amplification of the GH shift is achieved.

Following Aharonov-Albert-Vaidman’s (AAV) approach [1, 4], the amplified (weak values) GH shifts are given by:

$$x_{GH}^w = \frac{\langle \Psi_2 | \hat{X}_{GH} | \Psi_1 \rangle}{\langle \Psi_2 | \Psi_1 \rangle}. \quad (1)$$

The real and imaginary parts of the equation (1) correspond to spatial and angular GH shifts, respectively. The experimental set-up to observe the GH shift using a quantum weak measurement scheme is illustrated in figure 1. We consider a right-handed Cartesian reference frame attached to the beam with z representing the direction of propagation, y representing the vertical direction, and x fixed by the right-handed rule. As discussed before, the pre-selection, the post-selection, and the weak-coupling are the principal issues for implementing the weak measurement scheme. We fix the optic axis of the Glan-Thompson polarizer (GLP1) to an angle α to pre-select the incident light beam in a particular quantum state, which can be written as [7]:

$$e^{-\frac{x^2}{w^2}} \begin{pmatrix} \cos(\alpha) \\ \sin(\alpha) \end{pmatrix}. \quad (2)$$

Next, the light beam undergoes TIR from the prism (interaction with the system), which introduces a phase difference, producing state:

$$\begin{pmatrix} \cos(\alpha) \exp\left(-\frac{(x - D_p)^2}{w^2}\right) \exp\left(-i\frac{\delta}{2}\right) \\ \sin(\alpha) \exp\left(-\frac{(x - D_s)^2}{w^2}\right) \exp\left(+i\frac{\delta}{2}\right) \end{pmatrix} \quad (3)$$

where, $\delta = (\delta_p - \delta_s)$ is the phase difference between the p and s polarization components, D_p and D_s signify the GH shift introduced by the TIR of the light beam. Consequently, in the post-selection scheme, we apply a half-wave plate (HWP) and a quarter-wave plate (QWP). This combination is so adjusted to nullify the relative phase difference δ , if any. Finally, the optic axis of Glan-Thompson analyzer (GLP2) is rotated at an angle β to project out the final state:

$$\begin{pmatrix} \cos(\alpha) \cos(\beta) \exp\left(-\frac{(x - D_p)^2}{w^2}\right) \\ \sin(\alpha) \sin(\beta) \exp\left(-\frac{(x - D_s)^2}{w^2}\right) \end{pmatrix} \quad (4)$$

where, $\beta = (\alpha + \frac{\pi}{2}) + \varepsilon$

Following the approach of Duck [7], this state can finally be expressed as:

$$\frac{1}{2} \left[(1 + \varepsilon) \exp\left[-\frac{(x - \frac{1}{2}\Delta_{GH})^2}{w^2}\right] - (1 - \varepsilon) \exp\left[-\frac{(x + \frac{1}{2}\Delta_{GH})^2}{w^2}\right] \right] \quad (5)$$

where, we have taken $\tan(\varepsilon) \simeq \varepsilon$ and $\Delta_{GH} = (D_p - D_s)$.

For $\varepsilon = 0$, the above wave function clearly consists of two Gaussians centered at $x = \pm \Delta_{GH}/2$. The Gaussians are separated by approximately $\sqrt{2}w_0$ [2]. For $\Delta_{GH}/2w \ll \varepsilon \ll 1$, the two Gaussians will interfere constructively to produce a single Gaussian whose centroid is shifted by the weak value [2], $A_w \approx \frac{1}{2} \cot(\varepsilon) \Delta_{GH}$.

3. Experimental setup for QWM

In our experimental set-up, we have used 633 nm He-Ne laser (30991, Research Electro Optics Inc) as the source of light. It produces a good quality Gaussian light beam (Power 5.0 mW). The beam is then spatially filtered, collimated and focussed by a lens, L1 (LA1433, Thorlabs) of focal length 150 mm to a spot size w (250 μm). We control the polarization state of the incident light beam by using a Glan-Thompson Linear polarizer, GLP1 (GTH10M-A, Thorlabs) mounted on a high-precision rotational mount (PRM1/M,

Thorlabs). The beam then undergoes total internal reflection (TIR) from the surface of a 45°-90°-45° prism (N-BK7 RA, Thorlabs, refractive index, $n = 1.516$), mounted on a precision Rotation Stage (M-481-A, Newport). The post-selection unit consists of a combination of a quarter-wave plate, QWP (WPMQ10M-633, Thorlabs), a half-wave plate, HWP (WPMH10M-633, Thorlabs), followed by another Glan-Thompson Linear Polarizer, GLP2 (GTH10M-A, Thorlabs). They are all mounted on high precision Rotation Mounts (PRM1/M, Thorlabs). The resulting beam shift is subsequently monitored by a Beam Profiler, BP (LBP-4-USB, 6610d, Newport). We have also utilized a Polarimeter (PAX1000VIS/M, Thorlabs) to monitor the polarization state of the light beam in its path.

In conducting the experiment, atfirst, we have inspected the nature of the light beam using the beam profiler (BP) to verify its Gaussian nature, width, and power. Then, we pre-select the incoming beam to 45° linear polarization (LP) state by properly rotating the optic axis (α) of GLP1 and subsequently checking the output state with a Stokes Polarimeter (SP). After the total internal reflection (TIR) of this incident LP light from the prism, we post-select it by QWP & HWP. As mentioned in the theory section, we properly adjust the axis of QWP and HWP to a specific angle to compensate for the relative phase difference (δ). As the input polarization state of the beam is set at $\alpha = \pi/4$ using GLP1, we now adjust the output light beam to, $\beta = (\alpha + \pi/2) + \varepsilon$, ($\varepsilon \ll 1$) using GLP2 to achieve a nearly-orthogonal condition of weak measurement. The resultant beam, emerging out of the GLP2, is shifted by an amount ($\frac{1}{2}\Delta_{GH} \cot(\varepsilon)$). Next, we measure the separation of the beam centroids ($\Delta_{GH} \cot(\varepsilon)$) corresponding to two different polarization settings of, (1) $\alpha = \pi/4$ (pre-selection) and $\beta = (\alpha + \pi/2) + \varepsilon$ (post-selection) and, (2) $\alpha = \pi/4$ (pre-selection) and $\beta = (\alpha + \pi/2) - \varepsilon$ (post-selection).

4. Results and discussions

In the first stage of the experiment, we set GLP1 at $\alpha = \pi/4$, and GLP2 at $\beta = (\alpha + \pi/2) - \varepsilon$, and consequently varied ε ($0^\circ - 3^\circ$) by rotating GLP2 in small steps.

The resultant output has been shown in figure 2. Column (a) of figure 2 displays the output profiles of the resultant beam obtained from the beam profiler (BP). Column (b) and column (c) of figure 2 demonstrate the horizontal and the vertical patterns of the output beam, respectively. Figures 2(a5, b5 and c5) exhibits the resultant beam pattern for the case $\varepsilon \approx 0$ i.e. the case of exact orthogonality, where the AAV effect breaks down [1, 7]. As prescribed in the theory section, it is well justified here that the resultant beam splits into two separate Gaussian profiles separated by $\sqrt{2}w$ [2].

Figure 2 (upper panel (a4–a1)) depicts the behavior of the resultant beam output when ε is negatively increasing. In this case, the GLP2 is rotated in a clockwise sense from the orthogonal position. Subsequently, in figure 2, the lower panel (a6–a9) depicts the same when ε is positively increasing. In other words, the GLP2 is rotated anticlockwise from the orthogonal position. With increasing ε i.e. with increasing

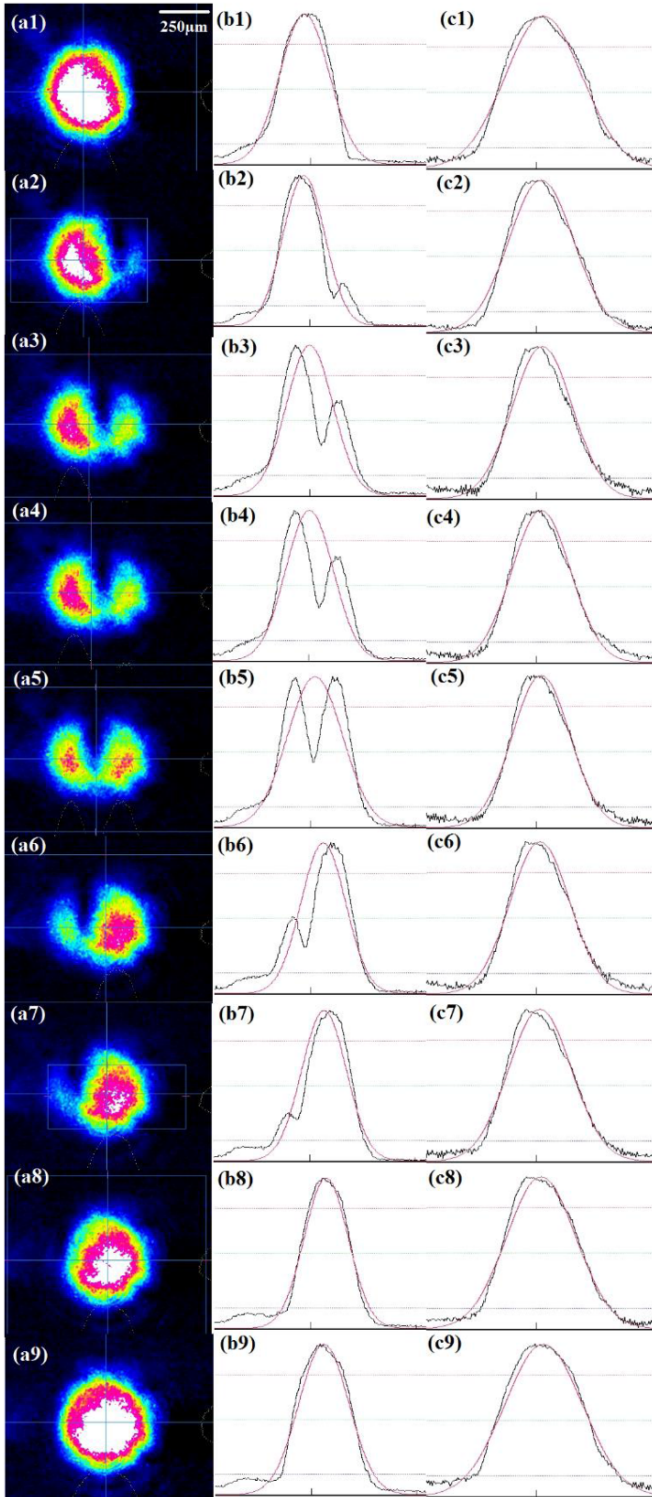


Figure 2. (a) Intensity of the beam centroid, (b) Horizontal, (c) Vertical distribution of the Intensity profile.

angular separation from the orthogonal position, one of the Gaussians becomes prominent, suppressing the other. These experimental observations support the concepts of weak measurement as proposed by AAV [1] and Duck [7].

Next, we have reported the behavior of the horizontal and vertical shifts of the output beam centroid as we move

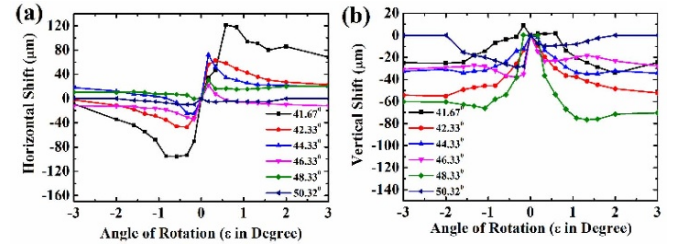


Figure 3. (a) Horizontal shift, (b) Vertical shift vs angle of rotation of GLP2.

away from the orthogonal position (by increasing ϵ) in both clockwise and anti-clockwise sense. The horizontal shift and vertical shift vs the angular deviation from the orthogonality are plotted in figures 3(a) and (b), respectively.

From figure 3(a) it is clear that as ϵ becomes non-zero, but is very close to zero, the shifts acquire a very large value. This is because of the breakdown of AAV approximation in close proximity of the orthogonal position, where $\langle \Psi_2 | \Psi_1 \rangle = 0$ blows up (equation (1)). As we move away from the orthogonal position, the horizontal shift starts decreasing in magnitude continuously, which is in accordance with AAV observations [1, 2, 7]. Another interesting fact is that the horizontal shift for positive ϵ is in the opposite sense compared to that for negative ϵ . This is obvious from the column (a, b) of figure 2. We can infer from figure 2, that for negative ϵ , the left-sided peak dominates and for positive ϵ , the right-sided peak dominates which are in agreement with our previous statement. We have also examined the horizontal shift for a different angle of incidence in the vicinity of the critical angle of incidence ($\theta_C = 41.6^\circ$ for glass-air interface). The horizontal shift has a much larger value in close proximity to the critical angle. But, as we move away from θ_C , the horizontal shift decreases sharply, which complies with previous theoretical observations [2, 7]. Meanwhile, as shown in figure 3(b), the vertical shift increases with ϵ , in contrast to the behavior of the horizontal shift. However, the increase in the vertical shift for positive ϵ and negative ϵ is in the same sense.

Next, we have studied the nature of the Goos-Hänchen (GH) shift for different angles of incidences of the incoming light beam on the prism. The results are plotted in figure 4(a). For a plane partial reflection of the light beam from the prism, no GH shift is observed. But for total internal reflection (TIR) of the light beam, a finite GH shift is obtained. In the vicinity of the critical angle of incidence, the GH shift exhibits giant values. This is also in agreement with the previous theoretical observations [27]. But as we recede away from θ_C , the GH shift monotonically decreases and with increasing θ , GH shift reaches zero level even in case of TIR.

Additionally, we have also investigated the variation of GH shift for different values of ϵ as described in figure 4(a). As ϵ is increased (moving away from orthogonality), the GH shift largely decreases for all angles of incidences. Finally, we have compared our experimental results of the GH shift with the theoretical values of the GH shift [28] as demonstrated in figure 4 (b). The experimental shifts match well with the

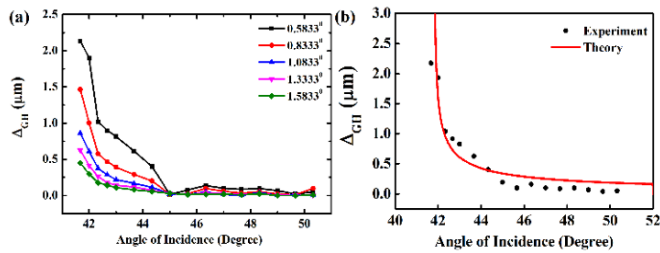


Figure 4. Variation of GH shift with the angle of incidence on the prism (a) varying ε , (b) comparing with theory.

theoretical values for a specific $\varepsilon = 0.5833^\circ/7' \approx 10^{-2}$ radian. This particular ε value provides a satisfactory amplification of the shift to be observed in accordance with the theoretical behavior without violating AAV approximation [1] of weak measurement.

5. Conclusions

In conclusion, we have experimentally investigated the optical Goos–Hänchen (GH) shift in total internal reflection (TIR) condition for a Gaussian light beam passing through a prism surface via quantum weak measurement (QWM) technique. We thoroughly described the profiles of the beam pattern and their behavior as one moves away from orthogonality. Our results clearly explain the region of validity of the AAV approximations for weak measurement in optics as an amplification scheme. The nature of the horizontal and vertical shift with non-zero ε depicts the exact nature of the shifts when the orthogonality condition is violated. Finally, we have prescribed how the GH shift for different angles of incidences depends highly on the selection of particular ε (angular deviation from orthogonal position) value. Our results demonstrate the advantages of the QWM technique for detecting tiny optical beam shift effects and open new possibilities for future applications in device industry and precision metrology.

Acknowledgments

AD and MP acknowledge the Technical Research Centre (No. All1/64/SNB/2014(C)) of S N Bose National Centre for Basic Sciences for providing the instrumental facilities. AD would gratefully thank the University Grant Commission (India) for PhD research fellowship.

References

- [1] Aharonov Y, Albert D Z and Vaidman L 1988 How the result of a measurement of a component of the spin of a spin-1/2 particle can turn out to be 100 *Phys. Rev. Lett.* **60** 1351–4
- [2] Ritchie N W M, Story J G and Hulet R G 1991 Realization of a measurement of a ‘weak value’ *Phys. Rev. Lett.* **66** 1107–10
- [3] Hosten O and Kwiat P 2008 Observation of the spin hall effect of light via weak measurements *Science* **319** 787–90
- [4] Aharonov Y and Rohrlich D 2005 *Quantum Paradoxes: Quantum Theory for the Perplexed* (New York: Wiley)
- [5] Ornigotti M and Aiello A 2013 Goos–Hänchen and Imbert–Fedorov shifts for bounded wavepackets of light *J. Opt.* **15** 014004
- [6] Töppel F, Ornigotti M and Aiello A 2013 Goos–Hänchen and Imbert–Fedorov shifts from a quantum-mechanical perspective *New J. Phys.* **15** 113059
- [7] Duck I M, Stevenson P M and Sudarshan E C G 1989 The sense in which a ‘weak measurement’ of a spin-1/2 particle’s spin component yields a value 100 *Phys. Rev. D* **40** 2112–17
- [8] Bliokh K Y and Aiello A 2013 Goos–Hänchen and Imbert–Fedorov beam shifts: an overview *J. Opt.* **15** 014001
- [9] Yin X, Hesselink L, Liu Z, Fang N and Zhang X 2004 Large positive and negative lateral optical beam displacements due to surface plasmon resonance *Appl. Phys. Lett.* **85**
- [10] Beenakker C W J, Sepkhanov R A, Akhmerov A R and Tworzydło J 2009 Quantum Goos–Hänchen effect in graphene *Phys. Rev. Lett.* **102** 146804
- [11] Zhou X, Ling X, Luo H and Wen S 2012 Identifying graphene layers via spin Hall effect of light *Appl. Phys. Lett.* **101** 251602
- [12] Chen S, Ling X, Shu W, Luo H and Wen S 2020 Precision measurement of the optical conductivity of atomically thin crystals via the photonic spin Hall effect *Phys. Rev. Appl.* **13** 014057
- [13] Mi C, Chen S, Wu W, Zhang W, Zhou X, Ling X, Shu W, Luo H and Wen S 2017 Precise identification of graphene layers at the air-prism interface via a pseudo-Brewster angle *Opt. Lett.* **42** 4135–8
- [14] Chen S, Mi C, Cai L, Liu M, Luo H and Wen S 2017 Observation of the Goos–Hänchen shift in graphene via weak measurements *Appl. Phys. Lett.* **110** 031105
- [15] Wang R, Zhou J, Zeng K, Chen S, Ling X, Shu W, Luo H and Wen S 2020 Ultrasensitive and real-time detection of chemical reaction rate based on the photonic spin Hall effect *APL Photonics* **5** 016105
- [16] Liu J, Zeng K, Xu W, Chen S, Luo H and Wen S 2019 Ultrasensitive detection of ion concentration based on photonic spin Hall effect *Appl. Phys. Lett.* **115** 251102
- [17] Aiello A 2012 Goos–Hänchen and Imbert–Fedorov shifts: a novel perspective *New J. Phys.* **14** 013058
- [18] Das A and Pradhan M 2018 Goos–Hänchen shift for Gaussian beams impinging on monolayer-MoS₂-coated surfaces *J. Opt. Soc. Am. B* **35** 1956–62
- [19] Resch K J 2008 Amplifying a tiny optical effect *Science* **319** 733–4
- [20] Dennis M R and Götte J B 2012 The analogy between optical beam shifts and quantum weak measurements *New J. Phys.* **14** 073013
- [21] Prajapati C, Pidishety S and Viswanathan N K 2014 Polarimetric measurement method to calculate optical beam shifts *Opt. Lett.* **39** 4388–91
- [22] Li X, W P, Xing F, Chen X-D, Liu Z-B and Tian J-G 2014 Experimental observation of a giant Goos–Hänchen shift in graphene using a beam splitter scanning method *Opt. Lett.* **39** 5574–7
- [23] Jayaswal G, Mistura G and Merano M 2013 Weak measurement of the Goos–Hänchen shift *Opt. Lett.* **38** 1232–4
- [24] Jayaswal G, Mistura G and Merano M 2014 Observation of the Imbert–Fedorov effect via weak value amplification *Opt. Lett.* **39** 2266–9

- [25] Götze J B and Dennis M R 2012 Generalized shifts and weak values for polarization components of reflected light beams *New J. Phys.* **14** 073016
- [26] Qin Y, Li Y, Feng X, Xiao Y-F, Yang H and Gong Q 2011 Observation of the in-plane spin separation of light *Opt. Express* **19** 9636–45
- [27] Das A and Pradhan M 2019 Exploring the optical beam shifts in monolayers of transition metal dichalcogenides using Gaussian beams *Opt. Commun.* **437** 312–20
- [28] Aiello A and W J P 2008 Role of beam propagation in goos–hänchen and imbert–fedorov shifts *Opt. Lett.* **33** 1437–9